

## Boundary spin disorder in nanocrystalline FeRh alloys

A. Hernando, E. Navarro,\* M. Multigner, and A. R. Yavari

*Instituto de Magnetismo Aplicado, Universidad Complutense, P.O. Box 155, Las Rozas 28230, Madrid, Spain*

D. Fiorani

*ICMAT CNR, Area della Ricerca di Roma, P.B. 10, 00016 Monterotondo Stazione, Italy*

M. Rosenberg

*Ruhr-Universität, Experimentalphysik VI, D-44780 Bochum, Germany*

G. Filoti

*IFTM, 76900-Bucharest, Romania*

R. Caciuffo

*Dipartimento di Scienze dei Materiali e della terra, University of Ancona, Ancona, Italy*

(Received 20 April 1998)

The magnetic properties of the ball-milled nanocrystalline fcc phase of FeRh alloys are reported and discussed. The observed features (maximum of ac and zero-field cooling susceptibility at a temperature  $T_{\max}$  weakly dependent on the frequency and on the applied field) suggest a progressive blocking of moments of nanograins with decreasing temperature, followed by their collective freezing in random directions at  $T_{\max}$ . The shifted hysteresis loop observed after field cooling as well as the remarkable irreversibility in high fields indicates that  $T_{\max}$  corresponds to the freezing temperature of the strongly deformed grain boundaries, which behave as a spin-glass-like phase. [S0163-1829(98)08633-0]

The magnetic properties of FeRh alloy<sup>1-3</sup> have been receiving a renewed interest in the last few years,<sup>4</sup> due to the variety of structural and magnetic phases exhibited depending on the composition, temperature, and preparation and processing methods. The Fe-Rh phase diagram indicates that FeRh alloys solidify as paramagnetic fcc solid solutions, but upon cooling, undergo a first-order transformation to paramagnetic ordered ( $B2$ ) bcc for compositions with more than 50 at. % Fe content. Upon further cooling, the Fe-rich paramagnetic ordered  $B2$  or ( $\alpha'$ ) compositions become ferromagnetic near 680 K. At still lower temperatures, usually below 400 K, a ferro-antiferromagnetic ( $\alpha' \rightarrow \alpha''$ ) transformation occurs in properly annealed samples in a range very close to  $\text{Fe}_{50}\text{Rh}_{50}$ .<sup>1</sup> It is also known that input of mechanical energy during milling (filing or rolling) transforms bcc FeRh compositions into the metastable state of the  $\gamma$ -fcc high-temperature solid solution, which is paramagnetic.<sup>2</sup> In this paper we report a low-temperature (down to 4.2 K) investigation of magnetic properties for a wide composition  $26 < x < 65$  range of  $\text{Fe}_x\text{Rh}_{100-x}$  nanocrystalline fcc alloys obtained by ball milling of the equilibrium phases. A maximum of the susceptibility is observed, and its nature is discussed.

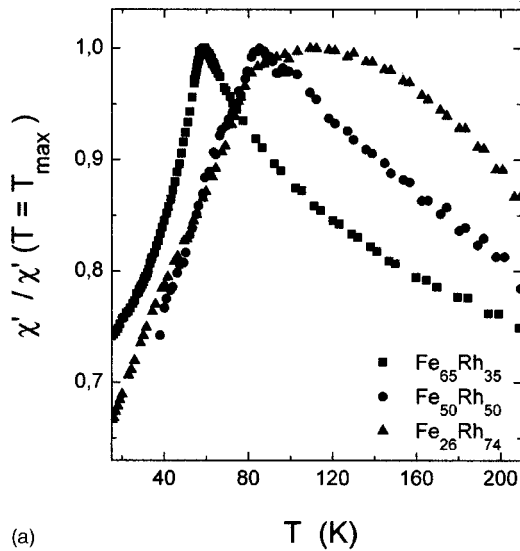
For the present study, four compositions were selected:  $\text{Fe}_{65}\text{Rh}_{35}$ , which corresponds to the middle of the ferromagnetic ordered bcc phase field, antiferromagnetic  $\text{Fe}_{50}\text{Rh}_{50}$ , which is also ordered bcc, and  $\text{Fe}_{28}\text{Rh}_{72}$  and  $\text{Fe}_{26}\text{Rh}_{74}$ , which are fcc and paramagnetic. Ingots were prepared by induction melting the pure components under pure argon gas, melt spun to reduce sample thickness, and subsequently ball milled into powder form. At each stage, phase identification was performed using a Siemens diffractometer with copper

$K\alpha$  radiation and in  $2\theta$  geometry. Magnetization and dc susceptibilities were measured in a commercial superconducting quantum interference device (SQUID) magnetometer (Quantum Design) and ac susceptibilities using a commercial susceptometer (Lakeshore). Mössbauer experiments were made with a conventional constant-acceleration spectrometer in a standard transmission geometry using a  $^{57}\text{Co}$  source in a Rh matrix.

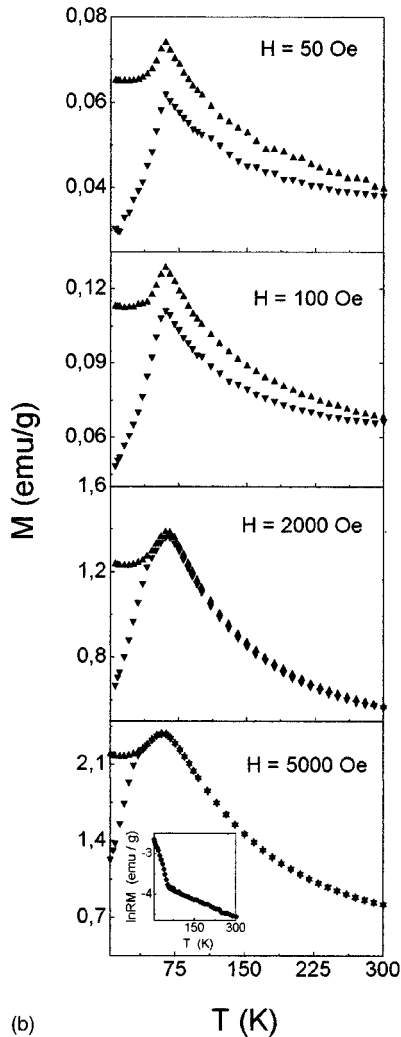
After ball milling, all four compositions are single phased. After severe deformation due to ball milling, Halder-Wagner<sup>5</sup> as well as Scherrer<sup>6</sup> peak profile analysis yielded an approximate coherent domain or grain size ranging from 9 to 17 nm with an increase in Rh content (Table I). This is consistent with the well-known fact that the lower limit of grain size increases with increasing ductility.<sup>7</sup> The samples were submitted to differential scanning calorimetry (DSC) analysis. As expected, the fcc to ordered bcc transformation is signaled by a large exothermic peak near 600 K for  $\text{Fe}_{65}\text{Rh}_{35}$  and  $\text{Fe}_{50}\text{Rh}_{50}$ , but not for  $\text{Fe}_{28}\text{Rh}_{72}$ , which is also fcc at equilibrium.

TABLE I. Average grain size ( $D$ ), maximum of the thermal dependence of real part of the ac susceptibility measured at 111 Hz ( $T_{\max}$ ), and shift of hysteresis loop after FC in a field of 2 T and at 5 K, for  $\text{Fe}_{65}\text{Rh}_{35}$ ,  $\text{Fe}_{50}\text{Rh}_{50}$ , and  $\text{Fe}_{26}\text{Rh}_{74}$ .

Compositions	$D$ (nm)	$T_{\max}$ (K)	Shift (Oe)
$\text{Fe}_{65}\text{Rh}_{35}$	8.6	59	1610
$\text{Fe}_{50}\text{Rh}_{50}$	13.2	85	500
$\text{Fe}_{26}\text{Rh}_{74}$	17.3	120	130



(a)



(b)

FIG. 1. (a) Real part of the ac susceptibility as a function of temperature of FeRh powders measured in a dc field of 100 A/m and frequency of 111 Hz. The values are normalized by the susceptibility at  $T = T_{\max}$ . (b) Magnetization vs temperature for different fields of ball-milled  $\text{Fe}_{65}\text{Rh}_{35}$  measured during heating after zero field cooling (ZFC,  $\blacktriangledown$ ) and field cooling (FC,  $\blacktriangle$ ). Inset: Remanent magnetization (after cooling down in a field of 100 Oe), as a function of temperature for  $\text{Fe}_{65}\text{Rh}_{35}$ .

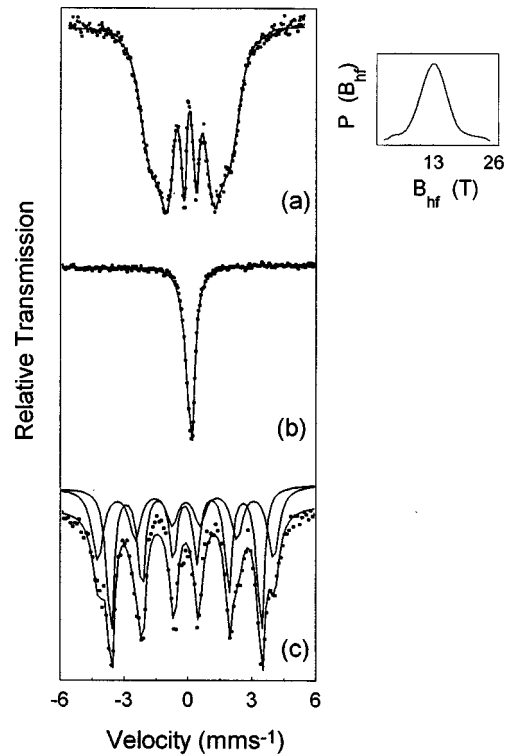


FIG. 2. Mössbauer spectra for  $\text{Fe}_{50}\text{Rh}_{50}$ : (a)  $T = 4.2$  K, (b)  $T = 300$  K, and (c) 475 K, and hyperfine field distribution at 4.2 K.

ac susceptibility [Fig. 1(a)] and magnetization [Fig. 1(b)] measurements in both zero-field cooling (ZFC) and field cooling (FC) regimes were performed. The temperature of the maximum,  $T_{\max}$ , of the ZFC magnetization depends weakly on the applied field, unlike the splitting temperature  $T_{\text{sp}}$  between the ZFC and FC branches, which strongly increases by decreasing the field. The observed maxima and irreversibility are typical either of a blocking of superparamagnetic moments or of a spin glass freezing. For  $\text{Fe}_{26}\text{Rh}_{74}$  the maximum is much broader. The  $\gamma$  phase of  $\text{Fe}_{50}\text{Rh}_{50}$  was also studied with Mössbauer spectroscopy. In Fig. 2(a) the 4.2 K Mössbauer spectrum is presented. It is similar to that of an amorphous magnet with a rather broad distribution of hyperfine fields around a quite low average value of 13.6 T, in good agreement with an earlier study of Sumiyama *et al.*<sup>8</sup> The spectrum measured at 300 K has a paramagnetic singlet [Fig. 2(b)]. The broad distribution of hyperfine fields can be due either to a distribution of relaxation times in superparamagnetic grains or to a spin glass state. At 475 K the metastable  $\gamma$   $\text{Fe}_{50}\text{Rh}_{50}$  phase transforms irreversibly into the stable bcc one [Fig. 2(c)]. The occurrence of the maximum in the susceptibility, the irreversibility, and the large distribution of hyperfine fields should be in principle correlated with the nanocrystalline structure induced by ball milling.

The increase of  $T_{\max}$  with Rh content corresponds also to an increase in grain size (Table I). It is therefore tempting to associate the occurrence of the maxima with a blocking of moments of nanosized superparamagnetic particles. But in the present case, for our polycrystalline samples, the grains are in contact and only separated by grain boundaries. In order to allow a superparamagnetic behavior, the grains have to be exchange decoupled. In such a case the maximum in

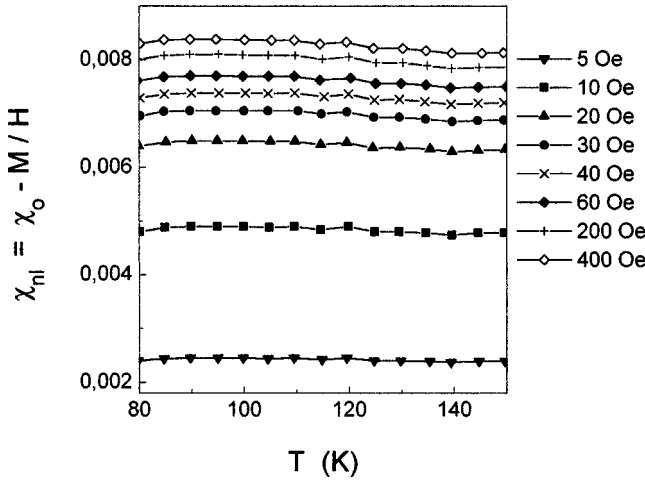


FIG. 3.  $\chi_{nl}$  vs temperature for different fields for  $\text{Fe}_{50}\text{Rh}_{50}$ .

the susceptibility could arise because of a blocking process of the superparamagnetic grains. In order to verify this possibility, we studied the frequency dependence of  $T_{\max}$  by measuring the real part of the ac susceptibility as a function of temperature at frequencies of 57, 111, 222, 333, 400, 500, 666, and 1000 Hz. The results indicate that this dependence is too small to be explained by the blocking of superparamagnetic moments. The frequency sensitivity of  $T_{\max}$ , usually taken as  $[T_{\max}(\nu_1) - T_{\max}(\nu_2)] / \{ \langle T_{\max} \rangle [\log_{10}(\nu_1) - \log_{10}(\nu_2)] \}$ , for  $\text{Fe}_{65}\text{Rh}_{35}$  ( $\nu_1$  and  $\nu_2$  being 1000 and 100 Hz, respectively), is 0.005, one or two orders of magnitude lower than that reported for weakly or noninteracting superparamagnetic particles, respectively,<sup>9</sup> and it is comparable to that reported for spin glasses.<sup>10</sup> Moreover, the very weak field dependence of  $T_{\max}$  is not compatible with a blocking temperature which is expected to clearly decrease with increasing field, due to the decrease of the anisotropy energy barrier.

In order to ascertain the occurrence of a pure spin glass transition characterized by its own order parameter, we have analyzed the temperature dependence of the nonlinear susceptibility (up to 150 K) of fcc  $\text{Fe}_{50}\text{Rh}_{50}$  measuring the FC magnetization as a function of temperature for different fields (5 Oe  $< H < 500$  Oe). In spin glasses,  $\chi_{nl}$  is expected to show a power law critical divergence  $\chi_{nl} \sim (T - T_f)^{-\gamma}$  due to the divergence of the correlation length.<sup>11</sup> The analysis was performed according to the Sherrington-Kirpatrick mean field model.<sup>12</sup> We considered a development in terms of  $\chi_0 H$  instead of  $H$ , introducing the real thermal variation of  $\chi_0$ .<sup>13</sup> Actually, no linear dependence is observed in the  $M/\chi_0 H$  versus  $(\chi_0 H)^2$  plots except for very low field values. These curves superpose for temperatures ranging from 60 to 150 K. Independently of the type of  $M$  expansion as a function of  $H$ , the behavior of the nonlinear susceptibility can be analyzed by plotting  $\chi_{nl} = \chi_0 - M/H$  as a function of temperature for different fields. Such plots of  $\chi_{nl}$ , as shown in Fig. 3, did not show any change with temperature, confirming the absence of the singular behavior in proximity of  $T_{\max}$ . Therefore all observations rule out the existence of a pure thermodynamic spin glass transition in fcc  $\text{Fe}_{50}\text{Rh}_{50}$ .

Since both superparamagnetic blocking and canonical spin glass freezing can be discarded as origins of the susceptibility maximum, a different mechanism associated with the

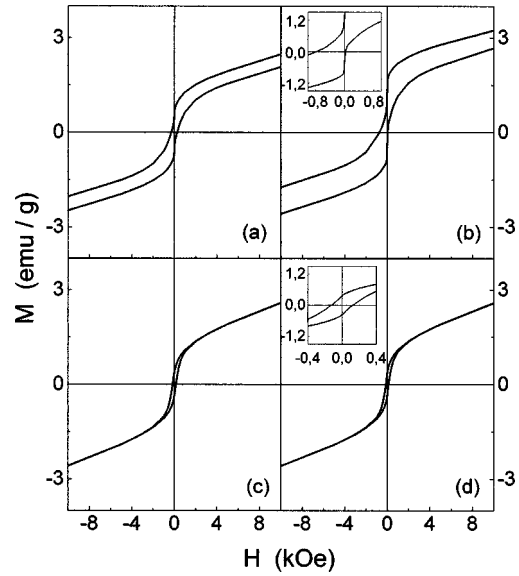


FIG. 4. Hysteresis loops for  $\text{Fe}_{50}\text{Rh}_{50}$  at  $T = 5$  K (a) after zero-field cooling and (b) after field cooling in a field of 2 T, and at  $T = 100$  K (c) after zero-field cooling and (d) after field cooling in a field of 2 T.

nanograin structure has to be considered. Magnetization curves and hysteresis loops were then measured and analyzed. The magnetization curves of  $\text{Fe}_{50}\text{Rh}_{50}$ , obtained below (5 K) and above  $T_{\max}$  (100 K) (see the hysteresis loops in Fig. 4), clearly include two contributions: one saturating at low fields and another varying linearly with the field. The latter one reveals the presence of antiferromagnetic interactions, whereas the first contribution indicates that the moments actually are not spontaneously compensated (as in a ferrimagnet) and can be oriented by the magnetic field. The magnetization due to the noncompensated moment is  $M_{nc} = 1.1$  emu/g, estimated by extrapolating to zero field the linear part of the magnetization at high fields.

In Figs. 4(b) and 4(d) the hysteresis loop obtained after cooling the sample in a field of 2 T is also reported. The most interesting result is the shifted hysteresis loop (shift of 500 Oe) observed after field cooling [Fig. 4(b)], which disappears at temperatures above  $T_{\max}$  [Fig. 4(d)]. For  $\text{Fe}_{65}\text{Rh}_{35}$  and  $\text{Fe}_{26}\text{Rh}_{74}$  compositions, the same behavior is observed. The shift of hysteresis loop (calculated from the difference between the coercivity fields of FC and ZFC curves) decreases as the grain size increases (Table I).

This effect, due to exchange anisotropy, is similar to that shown by oxide nanoparticles or oxide-coated nanoparticles<sup>14</sup> and by spin-valve systems.<sup>15</sup> The shifted hysteresis loop is well known to be due to the exchange coupling between antiferromagnetic (or spin glass) phases and ferromagnetic (or ferrimagnetic) phases. Moreover, the remarkable irreversibility in high field observed below  $T_{\max}$  [i.e., open hysteresis loops in Figs. 4(a) and 4(b) at least for fields below 5 T] indicate that the boundary spins have multiple configurations for any orientation of the grain magnetization. In our case the loop shift and the open hysteresis loops strongly indicate that the grain boundaries, which form the outer shell of the ferrimagnetic nanograins, behave as a spin-glass-like phase. The coexistence of both ferromagnetic and antiferromagnetic interactions in FeRh (Refs. 1 and 2) as

well as the broad distribution of interatomic distances in the highly deformed intergranular region<sup>16</sup> accounts for the spin-glass-like behavior.

It can be concluded that the presence of two magnetic regimes, below and above  $T_{\max}$ , is due to the spin-glass-like character of the intergranular region. At low temperature, the exchange between uncompensated moments of the nanograins, carried through the frozen moments of the boundaries, gives rise to a cluster glass arrangement. As the temperature rises, reaching the freezing temperature of the boundaries, the grains become uncoupled and the susceptibility reaches a maximum. The presence of a small rema-

nence [inset in Figs. 2(b) and 4(d)] up to temperatures much higher than  $T_{\max}$  clearly indicates that nanograin moments coexist in superparamagnetic and blocked states above  $T_{\max}$ . The increase of the freezing temperature of the boundary with increasing grain size indicates the influence of the structural disorder on the spin disorder [Fig. 1(a)]. A behavior similar to that reported in this paper is expected for other nanocrystalline samples in which ferromagnetic and antiferromagnetic interactions compete at the grain boundaries.<sup>16</sup> In particular, spin-glass-like and reentrant-spin-glass behavior observed for samples with anomalously high Fe content might be also due to the effects of the exchange anisotropy.<sup>17</sup>

\*Author to whom correspondence should be addressed. Fax: (+34)16301625. Electronic address:

JRODRIGUEZTORR@nexo.es, elena@fenix.ima.csic.es

<sup>1</sup>L. J. Swartzendruber, Bull. Alloy Phase Diagrams **5**, 1099 (1984); M. Fallot and R. Hocart, Rev. Sci. **77**, 498 (1939).

<sup>2</sup>J. M. Lommel and J. S. Kouvel, J. Appl. Phys. **38**, 126 (1967).

<sup>3</sup>V. L. Moruzzi and P. M. Marcus, Phys. Rev. B **46**, 2864 (1992).

<sup>4</sup>E. Navarro, A. R. Yavari, A. Hernando, C. Marquina, and M. R. Ibarra, Solid State Commun. **100**, 57 (1996).

<sup>5</sup>N. C. Halder and C. N. J. Wagner, Acta Crystallogr. **20**, 312 (1966).

<sup>6</sup>P. Scherrer, Nachr. Ges. Wiss. Göttingen **26**, 98 (1918).

<sup>7</sup>J. Eckert, J. C. Holzer, C. E. Krill, and W. L. Johnson, J. Appl. Phys. **73**, 2794 (1993).

<sup>8</sup>R. Sumiyama, M. Shiga, and V. Nakamura, Phys. Status Solidi A **1-3**, K75 (1972).

<sup>9</sup>J. L. Dormann, L. Bessais, and D. Fiorani, J. Phys. C **21**, 2015 (1988).

<sup>10</sup>C. A. M. Mulder, A. J. Van Duyneveldt, and J. A. Mydosh, Phys. Rev. B **23**, 1384 (1981).

<sup>11</sup>Clear evidence of a spin glass transition was found in dilute metallic alloys [e.g., Cu-Mn, R. Omari, J. Prejean, and J. Souletie, J. Phys. (Paris) **44**, 1069 (1983)] as well as in concentrated insulators where the frustration may be due either to a competition between ferromagnetic and antiferromagnetic interactions [e.g.,  $\text{Eu}_x\text{Sr}_{1-x}\text{S}$ , N. Bontemps, J. Rajchenbach, R. V. Chamberlin, and R. Orbach, J. Magn. Mater. **1**, 54 (1986);  $\text{CdCr}_{2-x}\text{In}_{2-2x}\text{S}_4$ , E. Vincent and J. Hammann, J. Phys. C **20**, 2659 (1987)] or a topological frustration in presence of antifer-

romagnetic interactions only [e.g.,  $\text{Y}_2\text{Mo}_2\text{O}_7$ , M. J. Gingras, C. V. Stager, N. P. Raju, B. D. Gaulin, and J. E. Gredan, Phys. Rev. Lett. **78**, 947 (1997)].

<sup>12</sup>D. Sherrington and S. Kirkpatrick, Phys. Rev. Lett. **35**, 1792 (1975).

<sup>13</sup>D. Fiorani, J. L. Tholence, and J. L. Dormann, J. Phys. C **19**, 5495 (1986).

<sup>14</sup>This effect is well known in ferrite nanoparticles and oxides. See, for instance, R. H. Kodama, Salah A. Makhlof, and A. E. Berkowitz, Phys. Rev. Lett. **79**, 1393 (1997); R. H. Kodama, A. E. Berkowitz, E. J. McNiff, Jr., and S. Foner, J. Appl. Phys. **81**, 5552 (1997).

<sup>15</sup>B. Dieny, V. S. Speriosu, S. S. P. Parkin, B. A. Gurney, D. R. Wilhoit, and D. Mauri, Phys. Rev. B **43**, 1297 (1991); See also Conference Digest of the 15th International Colloquium on Magnetic Films and Surfaces, Institute for Chemical Research, Kyoto University, 1997.

<sup>16</sup>It is interesting to note that in Ref. 14 the surface spin disorder of ferrites is explained by the sensitivity of superexchange to broken bonds. In our case the sample is metallic, but the high deformation of the boundary, also with broken bonds and a distribution of interatomic distances, should explain the coexistence of competitive interactions. A similar case has recently been analyzed in the boundary of nanocrystalline pure Fe. See, for instance, L. Del Bianco, A. Hernando, E. Bonetti, and E. Navarro, Phys. Rev. B **56**, 8894 (1997).

<sup>17</sup>G. F. Zhou and H. Bakker, Phys. Rev. Lett. **72**, 2290 (1994); **73**, 344 (1994).